Relevance of Newtonian seismic noise for the VIRGO interferometer sensitivity

M Beccaria†, M Bernardini†, S Braccini†, C Bradaschia†, A Bozzi†,
C Casciano†, G Cella‡¶, A Ciampa†, E Cuoco†§¶, G Curci†,
E D'Ambrosio†§, V Dattilo†, G De Carolis†, R De Salvo†, A Di Virgilio†,
A Delapierre†, D Enard†, A Errico†, G Feng†, I Ferrante§, F Fidecaro†§,
F Frasconi†, A Gaddi†, A Gennai†, G Gennaro†, A Giazotto†,
P La Penna†§, G Losurdo†‖, M Maggiore†, S Mancini†§, F Palla†,
H B Pan†, F Paoletti†, A Pasqualetti†, R Passaquieti†, D Passuello†,
R Poggiani†§, P Popolizio†, F Raffaelli†, S Rapisarda†, A Viceré† and
Z Zhang†

† Istituto Nazionale di Fisica Nucleare, Sez. di Pisa, Via Livornese 582/a, 56010, S Piero a Grado, Pisa, Italy
‡ GCTP Renaio, Lucca, Italy
§ Dipartimento di Fisica, Universita' degli Studi di Pisa, Pisa, Italy
‖ Scuola Normale Superiore, Pisa, Italy

Abstract. In this paper we analyse the noise level induced by changes in the mass density distribution around the Virgo interferometric antenna. These stochastic mass density fluctuations generate a gravitational field which couples directly to the mirrors of the optical apparatus, and it could be relevant if the planned final sensitivity of the Virgo interferometer is to be reached.

PACS numbers: 0480N, 0710F, 0150P, 0340K

1. Introduction

Seismographic measurements show that the ground is in continual motion, with amplitudes of the order of micrometres [1, 2]. Ground motion in the frequency range of 1–10 Hz is mainly produced by phenomena such as winds, local traffic, trains and so on.

Atmospheric cyclonic systems over the oceans produce fluctuations at lower frequencies, the so-called *micro-seismic background*. Its amplitude spectrum presents a peak which corresponds to the period of the ocean waves (12 s) and a larger one at a doubled frequency, while in the range of 1–10 Hz is a decreasing function which can be parametrized approximately as a power law [3].

The energy is transferred from the atmosphere to the ocean, and thence to the ocean floor. Next it is transmitted through the crust for long distances ($\sim 10^3$ km), mainly in the form of surface waves. Near the coasts there is also the contribution of sea waves breaking on the shore. It is important to note that the micro-seismic noise level reduces with depth,

¶ Authors to whom correspondence should be addressed.

because it is mainly transported by surface waves, guided waves in near-surface layers and multiple reflections in shallow layers [4, 11].

The mass density fluctuations produced by these micro-seismic waves induce a stochastic gravitational field which couples directly to the test masses of the interferometer and induce a noise (the so-called *Newtonian noise*) which we want to estimate.

The geometry of the apparatus is shown in figure 1. The test masses are located in the towers: in the Virgo apparatus a big effort has been spent on the isolation of these masses from the direct influence of seismic vibrations. This is obtained by using a chain of oscillators which reduces the amplitude of vibrations of frequency f at the suspension point by a factor $(f/f_0)^{-2}$ at each stage, where f_0 is the frequency of a single oscillator†.
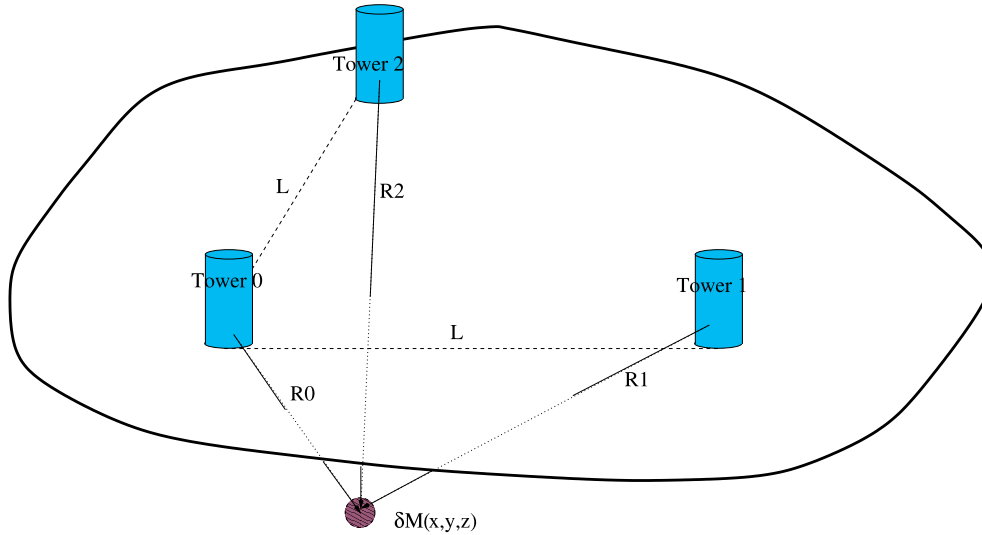
Figure 1. The schematic geometry used for the description of the interferometer.

(This figure can be viewed in colour in the electronic version of the article; see `http://www.iop.org`)

In the frequency range of interest we can describe the basis of a fixed attenuator as a rigid body with three translational modes (two horizontal and one vertical) and three rotational ones (a torsional mode around the attenuator axis and two 'tilt' modes). The chain of oscillators must provide attenuation for all these background vibration modes.

The fluctuating gravitational field couples to each stage of the chain, in particular (and this is the most relevant effect, as it bypasses all the attenuation stages) directly to the mirror [9]. The effect of a mass density fluctuation

$$\delta\rho(t) = \rho(t) - \langle\rho\rangle \tag{1}$$

located at a position $\boldsymbol{R}$ relative to the mirror on its displacement $\boldsymbol{x}$ can be written in the frequency space as

$$H(\omega)\,\boldsymbol{x}(\omega) = \frac{\boldsymbol{F}}{m} = G\,\delta\rho(\omega)\frac{\boldsymbol{R}}{R^3}\,\mathrm{d}V, \tag{2}$$

† This is true for frequencies higher than the resonances of the chain, which is the case for $f > 4$ Hz, and neglecting the internal modes of the structure which are relevant for high frequencies.

where $H(\omega)$ is the response function which connects the force applied to the system to its displacement†. If we assume that the mirror can be considered as a free test mass, which is the case far from the chain resonances, we have $H(\omega) = -\omega^2$.

The final effect we are interested in is the fluctuation of the relative difference $\delta h = \delta L/L$ between the optical paths in the two arms of the interferometer. This is connected to the displacement of the mirrors by a relation which depends on the geometrical structure of the apparatus. The simple scheme presented in figure 1 can be used to explain this point. In this model the variation of the optical path can be written as

$$\delta L = (r_{0,x} - r_{1,x}) - (r_{y,0} - r_{y,2}), \tag{3}$$

where $r_{1,i}, r_{2,i}$ are the coordinates of the mirrors and $r_{0,i}$ are those of the beamsplitter. Using the motion equation (2) this gives

$$H(\omega)\,\delta L(\omega) = \left(\frac{F_{0x}}{m} - \frac{F_{1x}}{m}\right) - \left(\frac{F_{0y}}{m} - \frac{F_{2y}}{m}\right) \tag{4}$$

and, explicitly,

$$H(\omega)\,\delta L(\omega) = G\,\delta\rho(\omega)\,K(x, y, z)\,dV, \tag{5}$$

$$K(x, y, z) = \left\{\frac{(L - y)}{\left(x^2 + (L - y)^2 + z^2\right)^{3/2}} - \frac{(L - x)}{\left((L - x)^2 + y^2 + z^2\right)^{3/2}} + \frac{(y - x)}{\left(x^2 + y^2 + z^2\right)^{3/2}}\right\}. \tag{6}$$

This expression is the starting point for our calculations. Note that the dependence on the geometrical structure of the interferometer is contained in the expression $K(x, y, z)$. For a given model of the background dynamics we can integrate over all the mass fluctuations and obtain a connection between the seismic noise power spectrum (which can be measured with relative ease) and the Newtonian noise.

In section 2 we give a detailed account of a simplified model introduced by Saulson [5, 6], which we extend with a numerical integration procedure. A more refined model is presented in subsection 2.1. In section 3 we write the equations which connect surface and volume fluctuations with gravitational ones using an elastic model based on the wave modes which are a solution of the elastic wave equation in a homogeneous half-space. The classification of these modes is presented in appendix A. In section 4 we estimate the effect of gravitational coupling between the mirror and some surrounding structures, and we end with some conclusions in section 5.
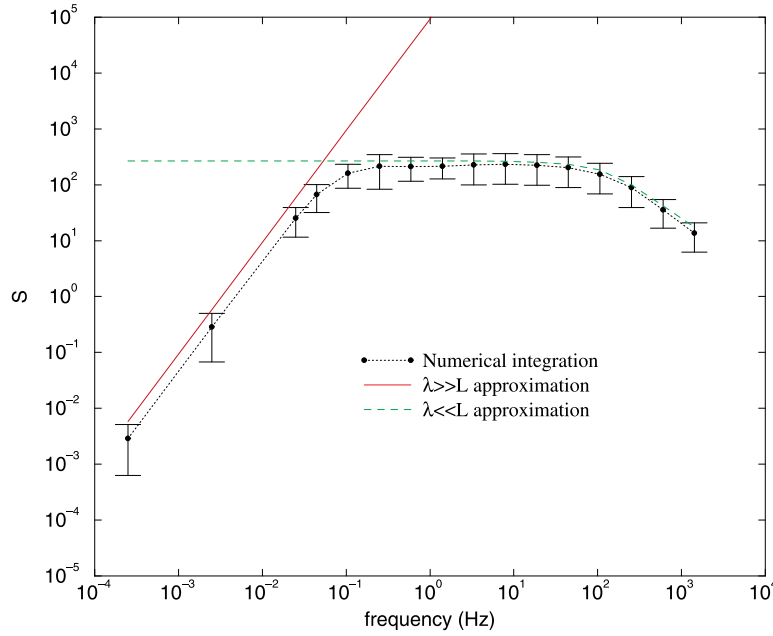
2. Saulson model

In this model [5] it is assumed that the density mass fluctuations of the ground are completely coherent over a characteristic scale $\lambda/2$, and completely uncorrelated for larger separations.

Fixing the attention over a cubic region of $(\lambda/2)^3$ volume centred on coordinates $(\bar{x}, \bar{y}, \bar{z})$, we must integrate equation (4) over this region, with $\delta M = \delta\rho(\lambda/2)^3$ fixed. The integral can be evaluated analytically, obtaining

$$H(\omega)\,\delta L(\omega) = G\,\delta M(\omega)\,B(\bar{x}, \bar{y}, \bar{z}) \tag{7}$$

---

† Note that in the general case R is a tensor. All the formulae which follow can be easily generalized to this case.

Figure 2. The function S defined in the text for Saulson's model. The full line represents the leading order in the high-wavelength approximation ($\lambda \gg L$), while the broken line corresponds to the low-wavelength approximation. The error bars are estimates of the model indeterminacy.

(This figure can be viewed in colour in the electronic version of the article; see `http://www.iop.org`)

where

$$B(\bar{x}, \bar{y}, \bar{z}) = \frac{8}{\lambda^3} \int_{\bar{x}-\lambda/4}^{\bar{x}+\lambda/4} \int_{\bar{y}-\lambda/4}^{\bar{y}+\lambda/4} \int_{\bar{z}-\lambda/4}^{\bar{z}+\lambda/4} K(x, y, z) \, dx \, dy \, dz \qquad (8)$$

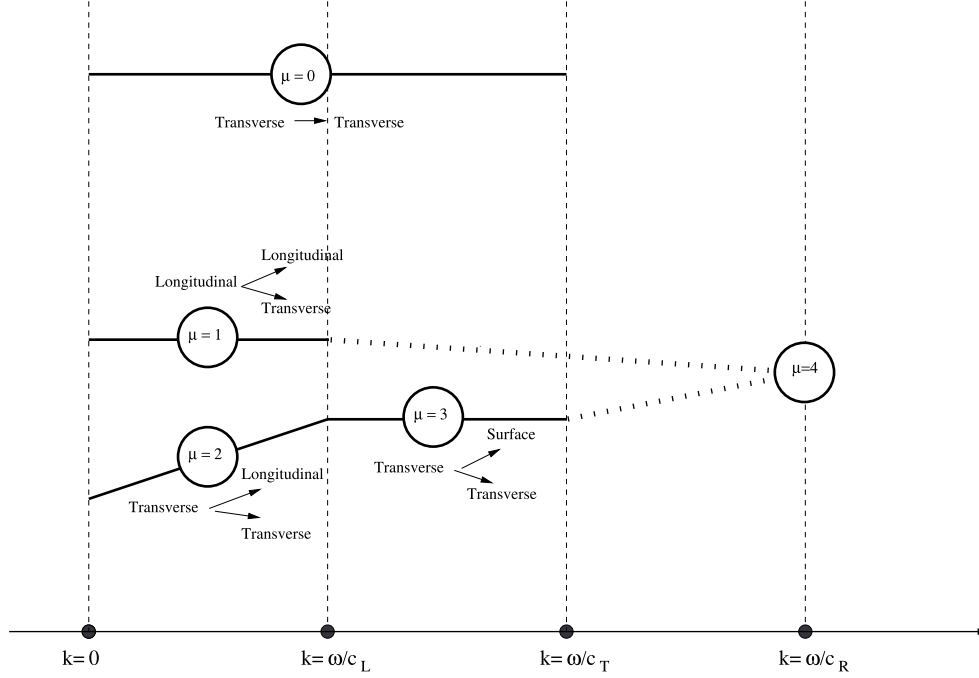is the mean value of the function K in the cell.

To obtain the total effect due to all the regions around the interferometer we sum in quadrature the expression (7) over all the cubes, obtaining

$$|H(\omega)|^2 \langle |\delta L(\omega)|^2 \rangle = G^2 \langle |\delta M(\omega)|^2 \rangle \sum_{\bar{x}, \bar{y}, \bar{z}} B(\bar{x}, \bar{y}, \bar{z})^2 = G^2 \langle |\delta M(\omega)|^2 \rangle \frac{1}{\lambda^4} S\left(\frac{\lambda}{L}, \frac{\lambda}{h}\right), \qquad (9)$$

which depends on the average of the square of the random cell fluctuation δM. We evaluate this sum numerically, using $L = 3000$ m, obtaining the results plotted in figure 2. There is an ambiguity in the model, related to the position of the central mirror with respect to the nearest cube, so the results are presented with error bars which give an idea of this systematic indeterminacy.

As we can see the results interpolate well between the analytically calculable asymptotic behaviours valid for $\lambda \ll L$

$$\sum_{\bar{x}, \bar{y}, \bar{z}} B(\bar{x}, \bar{y}, \bar{z})^2 \sim \theta(4h - \lambda) \frac{8\pi}{h} \frac{1}{\lambda^3} + \theta(\lambda - 4h) \frac{16}{3} \pi \left(\frac{2}{\lambda}\right)^4 \left[1 - 3\left(\frac{h}{\lambda}\right) + 8\left(\frac{h}{\lambda}\right)^3\right], \qquad (10)$$

Figure 3. Schematic view of elastic modes for a fixed ω value.

where h is the height of the mirror over the background, and for $\lambda \gg L$

$$\sum_{\bar{x},\bar{y},\bar{z}} B(\bar{x},\bar{y},\bar{z})^2 \sim \frac{192}{15}\pi\left(\frac{2L}{\lambda}\right)^2\left(\frac{2}{\lambda}\right)^4. \tag{11}$$

There is an evident crossover for $f \sim (c_L/4L)\sqrt{\frac{5}{3}}$† from a regime in which each mirror sees effectively different and completely uncorrelated cubes, to another in which coherence effects are dominant. In the large-λ limit each mirror fluctuates coherently in the same direction, so that $\delta L \sim 0$. Note that the small-λ limit is evaluated by approximating the sum with an integral, which is regularized with the small-distance cut-off $r_{min} = \lambda/4$. This is the same procedure used and discussed by Saulson, we have added the effect of the suspension point h only.

In this simple model the connection between mass fluctuation and displacement is not determined. We can connect the Newtonian noise to the spectrum for the displacement of a point in the ground using the relation between the mean square of mass fluctuations and the mean square of displacements

$$\langle|\delta M(\omega)|^2\rangle = V^2\langle|\delta\rho(\omega)|^2\rangle = \frac{1}{16}\lambda^6\rho_0^2\left(\frac{\pi}{\lambda}\right)^2\langle|\delta x(\omega)|^2\rangle, \tag{12}$$

which is valid for a compressional wave. Here we have assumed that the size of the coherent region is half the wavelength of the wave λ. In turn, λ is connected to the frequency by the relation

$$\lambda = 2\pi\frac{c_L}{\omega}. \tag{13}$$

† With the typical geological parameters around the interferometer $f \simeq 1$ Hz.

Alternatively we could, for example, identify the mean square of the displacements with the mean-square position of the centre of mass of two adjacent cells. These different procedures give numerical differences no greater than a factor two, especially in the $\lambda \ll L$ limit which is of interest for us in this context.

Putting together equations (12) and (9) we obtain

$$\langle |\delta L(\omega)|^2 \rangle = \frac{1}{16} \frac{G^2}{|H(\omega)|^2} \pi^2 \rho_0^2 S\left(\frac{\pi c_L}{L\omega}\right) \langle |\delta x(\omega)|^2 \rangle. \tag{14}$$

The typical longitudinal wave speed c_L in the ground of Cascina is around 1000 m s^{-1}, so we expect that coherence effects occur at a frequency below $\frac{1}{6}$ Hz. For higher values the function $S(\lambda/L)$ is very well approximated by its low-λ limit, so the final result is

$$\langle |\delta h(\omega)|^2 \rangle = \frac{16}{3} \frac{\pi^3}{L^2} \frac{G^2 \rho_0^2}{|H(\omega)|^2} \langle |\delta x(\omega)|^2 \rangle \tag{15}$$

or numerically, substituting $H(\omega) = -\omega^2$,

$$\langle |\delta h(f)|^2 \rangle^{1/2} = 1.2 \times 10^{-11} \frac{1}{f^2} \langle |\delta x(f)|^2 \rangle^{1/2}. \tag{16}$$

2.1. A more refined model

A limitation of the Saulson model is that it does not take into account mass conservation. It is assumed that the content of each cell can fluctuate independently, but this is not possible because, for example, a growing mass in a cube must be connected to an incoming mass flux from the neighbouring ones.

It is possible to improve the model using as statistical variables the mass fluxes ψ_i associated with the faces of the cells. The statistical independence of ψ_i variables is compatible with the mass conservation, and we can write

$$\frac{\mathrm{d}}{\mathrm{d}t} M(\bar{r}) = \sum_{i=x,y,z} \left(\psi_i\left(\bar{r} - \tfrac{1}{4}\lambda n_i\right) - \psi_i\left(\bar{r} + \tfrac{1}{4}\lambda n_i\right) \right) \tag{17}$$

so that the equation (7) becomes

$$i\omega H(\omega)\, \delta L(\omega) = G\, B(\bar{r}) \sum_{i=x,y,z} \left(\psi_i\left(\bar{r} - \tfrac{1}{4}\lambda n_i\right) - \psi_i\left(\bar{r} + \tfrac{1}{4}\lambda n_i\right) \right). \tag{18}$$

If we sum over all the cells, and calculate the average of the square of the result we obtain

$$\langle |\delta L(\omega)|^2 \rangle = \frac{G^2}{\omega^2 |H(\omega)|^2} \langle |\psi(\omega)|^2 \rangle \sum_{\bar{r},i} \left(B\left(\bar{r} + \tfrac{1}{2}\lambda n_i\right) - B(\bar{r}) \right)^2. \tag{19}$$

In the $\lambda \ll L$ limit we can approximate the sum with an integral and add in quadrature the four contributions in equation (4), so that†

$$\sum_{\bar{r},i} \left(B\left(\bar{r} + \tfrac{1}{2}\lambda n_i\right) - B(\bar{r}) \right)^2 \sim \frac{8}{\lambda} \int \frac{1 + 3\cos^2\theta \sin^2\phi}{r^6}\mathrm{d}V = \theta(4h - \lambda)\frac{2\pi}{h^3}\frac{1}{\lambda}$$

$$+ \theta(\lambda - 4h)\frac{128}{3}\pi\left(\frac{2}{\lambda}\right)^4\left[1 - \frac{15}{4}\left(\frac{h}{\lambda}\right) + 8\left(\frac{h}{\lambda}\right)^3\right]. \tag{20}$$

The average of the square of the random variable ψ can be connected in a simple way to the mean-square displacement x using the relation (17)

$$\langle |\psi(\omega)|^2 \rangle = \omega^2 \tfrac{1}{6}\pi^2 \rho_0^2 \left(\tfrac{1}{2}\lambda\right)^4 \langle |\delta x(\omega)|^2 \rangle \tag{21}$$

† We regulate the integral with the cut-off $r > \lambda/4$, as we have done in the last section.

and we get the final result

$$\langle |\delta h(\omega)|^2 \rangle = \frac{64}{9} \frac{\pi^3}{L^2} \frac{G^2 \rho_0^2}{\omega^4} \langle |\delta x(\omega)|^2 \rangle \tag{22}$$

which is slightly higher (by a factor of $\frac{4}{3}$) than the original estimate in equation (16), so that we can say that the two models are equivalent. This 'improved' model can be described using another point of view, by observing that the mass fluctuations in adjacent cells are correlated,

$$\langle \delta M(r)\, \delta M(r + kn_i) \rangle = \langle \delta M_{\text{Saulson}}^2 \rangle \left(\delta_{k,0} - \tfrac{1}{6}\delta_{k,1} \right). \tag{23}$$

We recognize that the mass conservation condition is equivalent to a generalization of Saulson's model in which a correlation between fluctuations in different cells is introduced.

3. Homogeneous elastic ground model

In order to obtain a more realistic estimate we now want to simulate the ground as a homogeneous medium limited by the $z = 0$ plane. The seismic noise can be expanded in elastic waves, which are solutions of the equation

$$\partial_t^2 u_i(x, t) = c_T^2 \partial_k \partial_k u_i(x, t) + \left(c_L^2 - c_T^2 \right) \partial_i \partial_k u_k(x, t). \tag{24}$$

These solutions correspond in an infinite medium to longitudinal waves with speed c_L and transverse ones with speed c_T. The field $u_i(x, t)$ represents the displacement of a point from its original position x in the direction i.

In appendix A we report a detailed classification of these elastic modes. The main result is that these can be labelled by the frequency ω, the projection $\vec{k}$ of the wavenumber in the $z = 0$ plane and a discrete index μ which counts the available branches. These results will be used in order to obtain, in a particular case, a connection between the Newtonian noise and an easily measurable seismic noise. However there is a way to connect, in the general case, the bulk dynamic with the surface one which avoids the classification of the modes. Performing a Fourier transform on the x, y, t variables we reduce equation (24) to an ordinary differential equation in the z variable. This means that there is a linear relation between the displacement $u_i(z)$ and a convenient number of boundary condition for it in $z = 0$. In other words, there is a three-rows, six-columns array $\mathcal{W}(z)$ which connects $u_i(z)$ with $u_i(0)$ and $\partial_z u_i(0)$. We will not compute this array explicitly, because all the results we need will be obtained as a byproduct of the mode classification, but we stress that a linear operator which connects Newtonian noise to surface seismic noise always exists.

In this homogeneous model the mass density fluctuations are generated by two mechanisms, which we now describe. First of all a longitudinal wave generates a volume variation proportional to the trace of the stress tensor:

$$\mathrm{d}V \to \mathrm{d}V(1 + u_{xx} + u_{yy} + u_{zz}). \tag{25}$$

We work in the linear approximation for the deformations, so the density fluctuation is

$$\delta\rho = -\rho_0(1 + u_{xx} + u_{yy} + u_{zz}) \tag{26}$$

and the gravitational field fluctuation in the mirror position $(0, 0, h)$ can be written as

$$\begin{pmatrix} \delta\vec{a} \\ \delta a_z \end{pmatrix} = G\rho_0 \int_{z<0} (\partial_x u_x + \partial_y u_y + \partial_z u_z) \frac{1}{\left(x^2 + y^2 + (h - z)^2 \right)^{3/2}} \begin{pmatrix} \vec{x} \\ z - h \end{pmatrix} \mathrm{d}V, \tag{27}$$

where the integration is extended to all the $z < 0$ space. Using the mode classification explicitly we obtain the expression

$$\partial_x u_x + \partial_y u_y + \partial_z u_z = \mathrm{i}\frac{\omega^2}{c_L^2}\big\{\alpha(k,\omega,\mu)\mathrm{e}^{\mathrm{i}k_L z} + \alpha'(k,\omega,\mu)\mathrm{e}^{-\mathrm{i}k_L z}\big\}\mathrm{e}^{\mathrm{i}kx - \mathrm{i}\omega t} \tag{28}$$

which depends on the amplitudes α, α' of the longitudinal waves only, as only for these modes is there a compression effect (see appendix A). All integrals can be calculated starting from

$$I(hk_L, hk) = \int_{z<-h} \mathrm{e}^{\mathrm{i}kx + \mathrm{i}k_L z}\big(x^2 + y^2 + z^2\big)^{-3/2}\,\mathrm{d}V = 2\pi\,\mathrm{e}^{\mathrm{i}hk_L}\,\mathrm{Ei}(-hk - \mathrm{i}hk_L) \tag{29}$$

and we obtain the final result in the (k_x, k_y, z, ω) space

$$\begin{pmatrix} \delta\vec{a} \\ \delta a_z \end{pmatrix} = 2\pi\,G\rho_0 \begin{pmatrix} \hat{k} \\ \mathrm{i} \end{pmatrix}(A_\mu k - \mathrm{i}B_\mu k_L)\mathrm{e}^{-hk}, \tag{30}$$

where $A = \alpha + \alpha'$ and $B = \alpha - \alpha'$. The second source of mass density fluctuations is given by the surface oscillations, which generate a mass density excess (positive or negative) that in the linear approximation can be written as

$$\mathrm{d}m = \rho_0\,u_z(x, y, 0)\,\mathrm{d}x\,\mathrm{d}y. \tag{31}$$

This must be integrated over all the $z = 0$ plane,

$$(\delta\vec{a}, \delta a_z) = G\rho_0 \iint \frac{(\vec{x}, -h)}{\big(x^2 + y^2 + h^2\big)^{3/2}}u_z(x, y, 0)\,\mathrm{d}x\,\mathrm{d}y. \tag{32}$$

We note that here only surface quantities are involved by definition. Using the mode classification with calculations analogous to those of the first case we obtain the final result

$$\begin{pmatrix} \delta\vec{a} \\ \delta a_z \end{pmatrix} = 2\pi\,\mathrm{i}G\rho_0 \begin{pmatrix} \hat{k} \\ \mathrm{i} \end{pmatrix}\left(\frac{k_T^2 + k^2}{k_T^2 - k^2}\right)k_L B_\mu\mathrm{e}^{-hk}. \tag{33}$$

Note that here and in the last section the height h of the test mass suspension point plays the role of a cut-off for small-wavelength modes.

3.1. Transfer function

One of our objectives is to understand the relation between the Newtonian noise spectrum and the seismic one. In order to do that we must write the influence of the elastic modes of the background over the interferometer infrastructures. We can model this effect simulating the base of the tower as a rigid body supported by the soil. This support is coupled to the deformations induced by the seismic waves. These alter the distances and the angles on the soil, and we can assume them to be coupled only to the internal deformations of the basement, so we neglect them assuming that they are decoupled from the relevant motions. On the other hand, if λ is large enough these can be described as a rigid motion of the basement: first of all two horizontal translations on the plane

$$\delta\vec{x} \to \vec{u}(\vec{x}) \tag{34}$$

and the vertical motion of the soil

$$\delta z \to u_z(\vec{x}) \tag{35}$$

which give rise to the horizontal and vertical seismic noise. Next we can consider the rotations of the basement, which can be written as

$$\delta\theta_z = \tfrac{1}{2}(\partial_x u_y - \partial_y u_x) \qquad \text{(torsional motion)} \tag{36}$$

$$\delta\theta_{\bar{x}} = \partial_{x,y} u_z \qquad \text{('tilt' motions).} \tag{37}$$

The relative contributions of the general elastic mode to these movements can easily be written using the classification reported in appendix A. We obtain

$$\delta\vec{x}(\vec{k}, z = 0, \omega) = \sum_\mu A_\mu(\vec{k}, \omega)\frac{\omega^2}{2c_T^2 k^2}\vec{k} + \sum_\mu C_\mu(\vec{k}, \omega)\epsilon\vec{k} \tag{38}$$

$$\delta z(\vec{k}, z = 0, \omega) = \sum_\mu B_\mu(\vec{k}, \omega)\frac{\omega^2}{c_T^2}\frac{k_L}{k_T^2 - k^2} \tag{39}$$

$$\delta\theta_{\bar{x}}(\vec{k}, z = 0, \omega) = \mathrm{i}\sum_\mu B_\mu(\vec{k}, \omega)\frac{\omega^2}{c_T^2}\frac{k_L}{k_T^2 - k^2}\vec{k} \tag{40}$$

$$\delta\theta_z(\vec{k}, z = 0, \omega) = \sum_\mu -\tfrac{1}{2}\mathrm{i}C_\mu(\vec{k}, \omega)k^2, \tag{41}$$

where we have Fourier transformed the x, y, t variables and $C = \gamma + \gamma'$, the amplitudes γ, γ' being defined in appendix A.

These relations can be solved with respect to the amplitudes A, B and C by separating $\delta\vec{x}$ and $\delta\theta_{\bar{x}}$ in a longitudinal and transverse part. The final result is

$$\sum_\mu A_\mu = 2\frac{c_T^2}{\omega^2}\vec{k} \cdot \delta\vec{x},$$

$$\sum_\mu B_\mu = \frac{c_T^2}{\omega^2}\left(\frac{k_T^2 - k^2}{k_L}\right)\delta z, \tag{42}$$

$$\sum_\mu C_\mu = \frac{2\mathrm{i}}{k^2}\delta\theta_z,$$

which shows that the amplitude A is connected to horizontal seismic noise, the amplitude B to the vertical seismic noise and the amplitude C to the torsional seismic noise. From equation (38) we can also get some relations that are model-independent kinematical consequences of definitions (34)–(37), for example the irrotationality of the tilt noise field, which is the gradient of the u_z field. It is easy now to connect the Newtonian acceleration to the seismic noise. Summing the volume and surface modes, which are given by expressions (30) and (33), we can write the contribution to the Newtonian acceleration generated by all the modes as

$$\begin{pmatrix}\delta\vec{a} \\ \delta a_z\end{pmatrix}(\vec{k}, z = h, \omega) = 2\pi G\rho_0\begin{pmatrix}\hat{k} \\ \mathrm{i}\end{pmatrix}\left\{k\sum_\mu A_\mu(\vec{k}, \omega) + 2\mathrm{i}\frac{k^2}{k_T^2 - k^2}k_L\sum_\mu B_\mu(\vec{k}, \omega)\right\}\mathrm{e}^{-hk}. \tag{43}$$

Using equation (38) we easily obtain the desired formula

$$\begin{pmatrix}\delta\vec{a} \\ \delta a_z\end{pmatrix}(\vec{k}, z = h, \omega) = 4\pi G\rho_0\frac{c_T^2}{\omega^2}\begin{pmatrix}\hat{k} \\ \mathrm{i}\end{pmatrix}\{k\vec{k} \cdot \delta\vec{x} + \mathrm{i}k^2\delta z\}\mathrm{e}^{-hk} \tag{44}$$

which gives a connection (transfer function) between seismic displacements measurable on the surface and the Newtonian force. This is the expected linear relation between Newtonian

noise and surface seismic noise, that with the boundary condition we choose, depends only on the longitudinal part of horizontal noise and on the vertical one.

If we transform back this relation in the x, y, z space we obtain an integral relation which can be written as

$$\begin{pmatrix} \delta\vec{a} \\ \delta a_z \end{pmatrix}(\vec{r}, z = h, \omega) = 2G\rho_0 \frac{c_T^2}{\omega^2} \int \begin{pmatrix} \overleftrightarrow{K}(\vec{r} - \vec{r}') & \vec{K}(\vec{r} - \vec{r}') \\ \vec{K}(\vec{r} - \vec{r}') & K(\vec{r} - \vec{r}') \end{pmatrix} \begin{pmatrix} \delta\vec{x} \\ \delta z \end{pmatrix}(\vec{r}', \omega)\, \mathrm{d}^2 r' \tag{45}$$

where

$$\begin{pmatrix} \overleftrightarrow{K}(\vec{r}) & \vec{K}(\vec{r}) \\ \vec{K}(\vec{r}) & K(\vec{r}) \end{pmatrix} = \begin{pmatrix} -\partial_{\vec{r}}\partial_{\vec{r}} & \partial_{\vec{r}}\partial_h \\ \partial_{\vec{r}}\partial_h & -\partial_h\partial_h \end{pmatrix} \frac{h}{\left(h^2 + r^2\right)^{3/2}}. \tag{46}$$

Equation (46) says that Newtonian noise is connected in a non-local way to the surface seismic noise, as it is expected. It is the 'transfer function' between seismic and Newtonian noise in its more general form for the elastic homogeneous model.

In order to obtain a more usable expression we need some additional information on the spatial dependence of seismic displacements. Our model gives us little information about this. In the general case we only know that, for a given frequency, there is a high momentum cut-off, so that the spatial dependence of seismic noise is somewhat 'smoothed'.

3.2. Noise power spectrum

In the last section we viewed the seismic and Newtonian noises as if they were standard functions of the time. As they are really stochastic processes we do not expect that quantities as their Fourier transform in the frequency domain possess any significance, without some suitable regularization. However, we can define some quantities which preserve their validity after removing this regularization, such as for example the two-point correlation

$$C_{x_1 x_2}(t, \vec{r}_1; t, \vec{r}_2) = \langle x(t, \vec{r}_1)\, x(t, \vec{r}_2)\rangle. \tag{47}$$

The precise definition of the $\langle\cdots\rangle$ average requires a careful study of the statistical properties of seismic noise, especially from the point of view of stationarity, and will not be given here. For a stationary, ergodic process we can operatively estimate C as an ensemble average of time limited measurements, and we can introduce the concept of a cross spectrum $S_{x_1 x_2}$ as the Fourier transform in time of $C_{x_1 x_2}$. Now if we rewrite equation (44) in the form

$$\begin{pmatrix} \delta\vec{a} \\ \delta a_z \end{pmatrix}(\vec{k}, \omega) = \boldsymbol{T}(\vec{k}, \omega) \begin{pmatrix} \delta\vec{x} \\ \delta z \end{pmatrix}(\vec{k}, \omega) \tag{48}$$

and if we assume translation invariance for seismic noise correlations, we get

$$\begin{pmatrix} S_{\vec{a}\vec{a}}(\vec{k}, \omega) & S_{\vec{a}a_z}(\vec{k}, \omega) \\ S_{a_z\vec{a}}(\vec{k}, \omega) & S_{a_z a_z}(\vec{k}, \omega) \end{pmatrix} = \boldsymbol{T}(\vec{k}, \omega) \begin{pmatrix} S_{\vec{x}\vec{x}}(\vec{k}, \omega) & S_{\vec{x}z}(\vec{k}, \omega) \\ S_{z\vec{x}}(\vec{k}, \omega) & S_{zz}(\vec{k}, \omega) \end{pmatrix} \boldsymbol{T}^+(\vec{k}, \omega) \tag{49}$$

which relate seismic noise cross spectra to Newtonian noise ones.

Our objective is to construct a relation between the Newtonian power spectrum and the seismic one, which is easily measurable. We can understand the information our model gives us about the r dependence of cross spectra writing them as a function of the unknown amplitudes A, B, C. We can discuss the main point fixing our attention on the vertical noise

cross spectrum, which can be written as†

$$S_{zz}(\vec{r}, \omega) = \frac{\omega^4}{c_T^4} \int \frac{k_L}{k_T^2 - k^2} \langle |B_\mu(\omega, \vec{k})|^2 \rangle e^{-i\vec{k}\cdot\vec{r}} \frac{d^2 k}{(2\pi)^2}$$

$$= \frac{\omega^4}{c_T^4} \int \frac{k k_L}{k_T^2 - k^2} \langle |B_\mu(\omega, k)|^2 \rangle J_0(kr) \frac{dk}{2\pi}. \tag{50}$$

As we mentioned at the end of the last section, the only general conclusion is that the cross spectrum S is a smooth function of r. We need to measure the spatial dependence of S in order to estimate the B amplitude.

A less expensive solution is to make some additional assumptions in our model, in particular, we can suppose that the only relevant modes are the Rayleigh ones. This is a strong statement, but it is somewhat physically motivated because surface waves are strongly localized near the surface, so their effect is maximized. In addition, they are the most efficient mechanism for energy transport from the far micro-seismic noise sources location.

The main consequence of our hypothesis is that the wavenumber is fixed by the frequency, so that equation (43) becomes

$$\begin{pmatrix} \delta\vec{a} \\ \delta a_z \end{pmatrix} = G\rho_0 W(\xi) \begin{pmatrix} \hat{k} \\ i \end{pmatrix} A_4(\hat{k}, \omega) \frac{\omega}{c_T} \exp\left(-h\frac{\omega}{c_T\sqrt{x}}\right). \tag{51}$$

where the W is a function of the c_T/c_L ratio (see equations (A11) and (A12))

$$W(\xi) = 2\pi \left\{ \frac{1}{\sqrt{x}} + \frac{2}{x-2}\sqrt{\frac{1}{x} - \xi} \right\}. \tag{52}$$

We used the relation between the A and B amplitudes valid for the Rayleigh modes (see appendix A).

Now we can evaluate the cross spectra. The key assumption of our model is that the random amplitudes connected to different elastic modes are statistically uncorrelated. If we also assume that the autocorrelation function is isotropic the double sum over modes reduces to an angular integral which can be evaluated in terms of Bessel functions. In this way it is possible to evaluate the correlations between longitudinal accelerations, or the mixed longitudinal–transverse ones, with the final result

$$\langle \delta a_i(x_1)\, \delta a_j(x_2) \rangle = \frac{1}{2} G^2 \rho_0^2 \left(\frac{\omega}{c_T}\right)^2 W^2 \langle |A_4(\omega)|^2 \rangle G_{ij}^T(\vec{x}_1, \vec{x}_2) \exp\left(-2h\frac{\omega}{c_T\sqrt{x}}\right) \tag{53}$$

$$\langle \delta a_i(x_1)\, \delta a_z(x_2) \rangle = \frac{1}{2} G^2 \rho_0^2 \left(\frac{\omega}{c_T}\right)^2 W^2 \langle |A_4(\omega)|^2 \rangle G_i^V(\vec{x}_1, \vec{x}_2) \exp\left(-2h\frac{\omega}{c_T\sqrt{x}}\right) \tag{54}$$

$$\langle \delta a_z(x_1)\, \delta a_z(x_2) \rangle = \frac{1}{2} G^2 \rho_0^2 \left(\frac{\omega}{c_T}\right)^2 W^2 \langle |A_4(\omega)|^2 \rangle G^S(\vec{x}_1, \vec{x}_2) \exp\left(-2h\frac{\omega}{c_T\sqrt{x}}\right). \tag{55}$$

The functions $G(\vec{x}_1, \vec{x}_2)$ are the results of the sum over modes, and are defined in appendix B. As we can see the effect is exponentially damped with the height of the suspension point, with a characteristic length which is inversely proportional to the frequency.

Using the relation (4) we can write the spectrum of the noise generated by the Newtonian forces for the simple interferometer geometry depicted in figure 1 as

$$\langle |\delta L(\omega)|^2 \rangle = \frac{1}{|H(\omega)|^2} \langle |\delta a_x(0) + \delta a_y(2) - \delta a_x(1) - \delta a_y(0)|^2 \rangle \tag{56}$$

† The last equality is true if we assume isotropy.
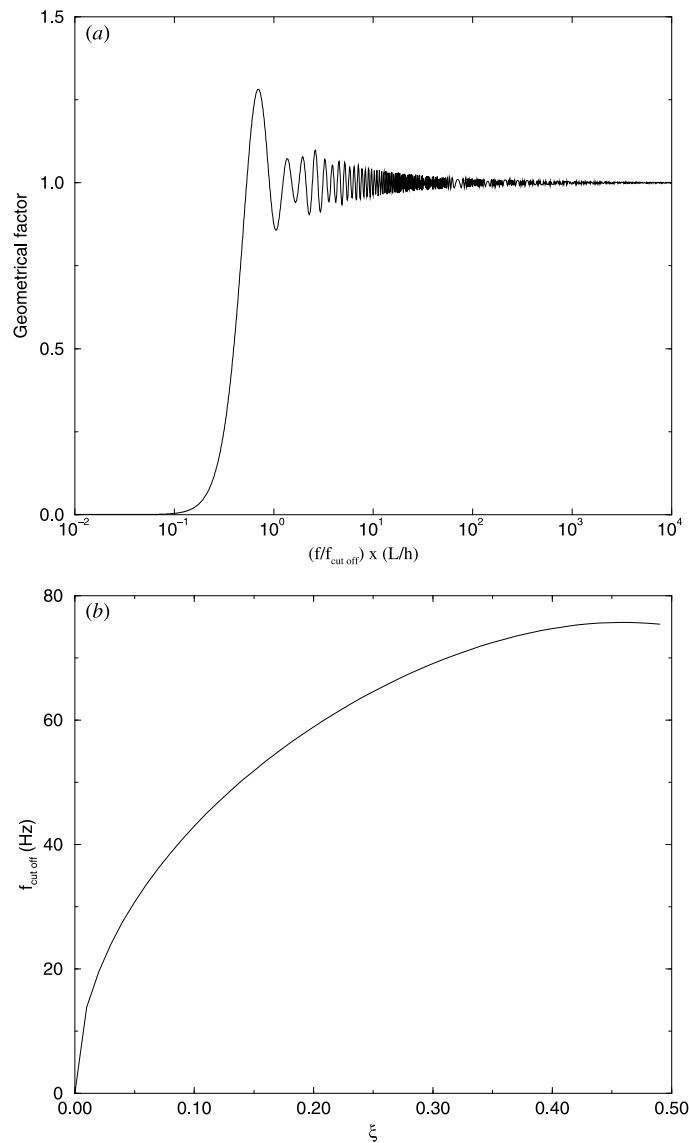
Figure 4. (*a*) The geometrical factor $\mathcal{G}$ for the simple interferometer geometry considered. (*b*) The cut-off frequency dependence on the ξ ratio, for a fixed longitudinal speed of 1000 m s^{-1}.

which can be expanded as a sum of two-point correlation functions and rewritten in the final form as

$$\langle |\delta L(\omega)|^2 \rangle = 2\pi \frac{G^2 \rho_0^2}{|H(\omega)|^2} \left(\frac{\omega}{c_T} \right)^2 |W|^2 \langle |A_4(\omega)|^2 \rangle \exp\left(-\frac{2h\omega}{c_T \sqrt{x}} \right) \mathcal{G}\left(\frac{\omega L}{c_T \sqrt{x}} \right) \tag{57}$$

with

$$\mathcal{G}(t) = 1 - J_0(t) - J_2(t) - \tfrac{1}{2} J_2\left(t\sqrt{2} \right). \tag{58}$$

This geometric factor is depicted in figure 4(*a*). The correlations of seismic displacements can be evaluated in the same way. We can rewrite the relations (38) as

$$\delta\vec{x} = \frac{\omega\sqrt{x}}{2c_T}A_4(\omega,\hat{k})\hat{k} = \frac{\omega}{c_T}u_X A_4(\omega,\hat{k})\,\hat{k} \tag{59}$$

$$\delta z = \mathrm{i}\frac{\omega}{c_T}\frac{\sqrt{x(1-x\xi)}}{(2-x)}A_4(\omega,\hat{k}) = \frac{\omega}{c_T}u_Z A_4(\omega,\hat{k}) \tag{60}$$

$$\delta\theta_{\bar{x}} = -\frac{\omega^2}{c_T^2}\frac{\sqrt{1-x\xi}}{(2-x)}A_4(\omega,\hat{k})\hat{k} = \left(\frac{\omega}{c_T}\right)^2 u_\theta A_4(\omega,\hat{k})\,\hat{k} \tag{61}$$

$$\delta\theta_z = 0. \tag{62}$$

The quantities u_X, u_Z, u_θ defined by the relations above, are like W constants which depend only on the longitudinal and transverse sound speed. Squaring and summing over all the directions we find

$$\langle\delta x_i(x_1)\,\delta x_j(x_2)\rangle = \pi\left(\frac{\omega}{c_T}\right)^2|u_X|^2\langle|A_4(\omega)|^2\rangle G_{ij}^T(\vec{x}_1,\vec{x}_2) \tag{63}$$

$$\langle\delta z(x_1)\,\delta z(x_2)\rangle = \pi\left(\frac{\omega}{c_T}\right)^2|u_Z|^2\langle|A_4(\omega)|^2\rangle G^S(\vec{x}_1,\vec{x}_2) \tag{64}$$

$$\langle\delta\theta_i(x_1)\,\delta\theta_j(x_2)\rangle = \pi\left(\frac{\omega}{c_T}\right)^4|u_\theta|^2\langle|A_4(\omega)|^2\rangle G_{ij}^T(\vec{x}_1,\vec{x}_2) \tag{65}$$

and the mixed correlations

$$\langle\delta x_i(x_1)\,\delta z(x_2)\rangle = \pi\left(\frac{\omega}{c_T}\right)^2\mathrm{Re}\,(u_X^\star u_Z)\langle|A_4(\omega)|^2\rangle G_i^V(\vec{x}_1,\vec{x}_2) \tag{66}$$

$$\langle\delta x_i(x_1)\,\delta\theta_j(x_2)\rangle = \pi\left(\frac{\omega}{c_T}\right)^3\mathrm{Re}\,(u_X^\star u_\theta)\langle|A_4(\omega)|^2\rangle G_{ij}^T(\vec{x}_1,\vec{x}_2) \tag{67}$$

$$\langle\delta\theta_i(x_1)\,\delta z(x_2)\rangle = \pi\left(\frac{\omega}{c_T}\right)^3\mathrm{Re}\,(u_Z^\star u_\theta)\langle|A_4(\omega)|^2\rangle G_i^V(\vec{x}_1,\vec{x}_2). \tag{68}$$

Note that, owing to the presence of the Rayleigh modes only and the isotropy hypothesis, the spatial dependence of the correlations are completely fixed by their transformation properties under rotations.

The unknown function $\langle|A_4(\omega)|^2\rangle$, which sets the scale for the different noises in our model, can be eliminated by expressing all the quantities we are interested in with respect to one of them. We choose the transverse seismic power spectrum noise, which can be easily measured, and we write

$$\langle|A_4(\omega)|^2\rangle = \frac{2}{\pi}\left(\frac{c_T}{\omega}\right)^2\frac{1}{|u_X|^2}\langle\delta x_i(\omega)^2\rangle. \tag{69}$$

Using equation (57) we can write the relation which connects the Newtonian noise spectrum to the seismic one

$$\langle|\delta L(\omega)|^2\rangle = \frac{4G^2\rho_0^2}{|H(\omega)|^2}\frac{|W|^2}{|u_X|^2}\exp\left(-\frac{2h\omega}{c_T\sqrt{x}}\right)\mathcal{G}\left(\frac{\omega L}{c_T\sqrt{x}}\right)\langle\delta x_i(\omega)^2\rangle. \tag{70}$$

The exponential term cuts the Newtonian noise at high frequencies, and becomes relevant when the inverse wavelength of the seismic modes is comparable with the mirror–background distance h. In terms of the frequency the cut-off is effective when

$$\omega > \omega_{\mathrm{cut\text{-}off}} = \frac{c_L}{h}\sqrt{x\xi}. \tag{71}$$

For a fixed longitudinal wave speed $\omega_{\text{cut-off}}$ depends on the speed of transverse waves c_T as represented in figure 4(*b*). We see that the cut-off cannot be greater that 80 Hz, and is smaller for materials with a low transverse shear module.

The factor $\mathcal{G}$ is connected to the apparatus geometry, and describes the coherence effects. It is a function that initially grows as a fourth power at low frequency, and next is approximately one for frequencies greater than $10^{-3} f_{\text{cut-off}}$ (see figure 4(*a*)). It is generated by the interference of the noises at different mirrors, which for an inverse wavelength of the elastic mode comparable with the interferometer length is coherent and does not couple to the difference between the optical paths in the arms of the interferometer.

The ratio between the square amplitudes $|W|^2$ and $|u_X|^2$ depends on the speeds of sound for transverse and longitudinal waves (see table 1), and is included in the range between ~ 130 (low-shear modulus) and ~ 26 (high-shear modulus).

Table 1. The amplitudes of different noise sources for selected values of ξ, in the model with only Rayleigh modes.

ξ	x	$|u_X|^2$	$|u_Z|^2$	$|u_\theta|^2$	$|W|^2$
0.05	0.906 341	0.056 6463	0.723 415	0.798 17	26.965 3
0.10	0.899 137	0.056 1961	0.675 216	0.750 959	23.600 9
0.15	0.890 805	0.055 6753	0.627 299	0.704 193	20.391 7
0.20	0.881 076	0.055 0673	0.579 731	0.657 98	17.352 9
0.25	0.869 605	0.054 3503	0.532 599	0.612 461	14.502 4
0.30	0.855 931	0.053 4957	0.486 017	0.567 823	11.859 8
0.35	0.839 449	0.052 4655	0.440 138	0.524 318	9.447 16
0.40	0.819 359	0.051 2099	0.395 16	0.482 28	7.288 24
0.45	0.794 622	0.049 6639	0.351 345	0.442 153	5.406 82
0.50	0.763 932	0.047 7458	0.309 017	0.404 508	3.823 89

We are now in the position to discuss our final results. In figure 5 we have plotted the numerical values of the ratio between the transverse seismic noise spectral amplitude and the Newtonian noise spectral amplitude for the elastic and Saulson models, defined as the square root of the following quantity:

$$\frac{S_{hh}}{S_{xx}}(\omega) = \left|\frac{\delta L(\omega)}{L}\right|^2 \langle \delta x_i(\omega)^2\rangle^{-1}. \tag{72}$$

As a preliminary comment note that all the curves are constructed assuming that the mirror can be described as a free test mass, i.e. they are normalized to $H(\omega) = -\omega^2$. This is certainly not the case in the low-frequency region, but the effect of $H(\omega)$ is factorized (see, for example, equation (70)) and more detailed predictions can be easily obtained.

It is apparent that in the 0.1–50 Hz frequency range all the models give estimates of the same order of magnitude, with a transfer function which scales as the inverse square of the frequency. Our elastic model estimate is somewhat larger than Saulson's in this region.

Below 0.1 Hz the coherence effects are apparent. For Saulson's model the transfer function scales as the inverse first power of the frequency (see also figure 2), while in the elastic model the ω^{-2} factor which comes from the free mass dynamics is compensated by the ω^2 low-frequency behaviour of the geometrical factor.

In the high-frequency region ($f > 50$ Hz) the behaviour of the transfer function is determined by the height of the mirror's suspension point. However, for Saulson's model the influence of h is small, and generates only a small increase of the curve slope which starts to scale as $\omega^{-5/2}$. For the elastic model the effect is much more important, and
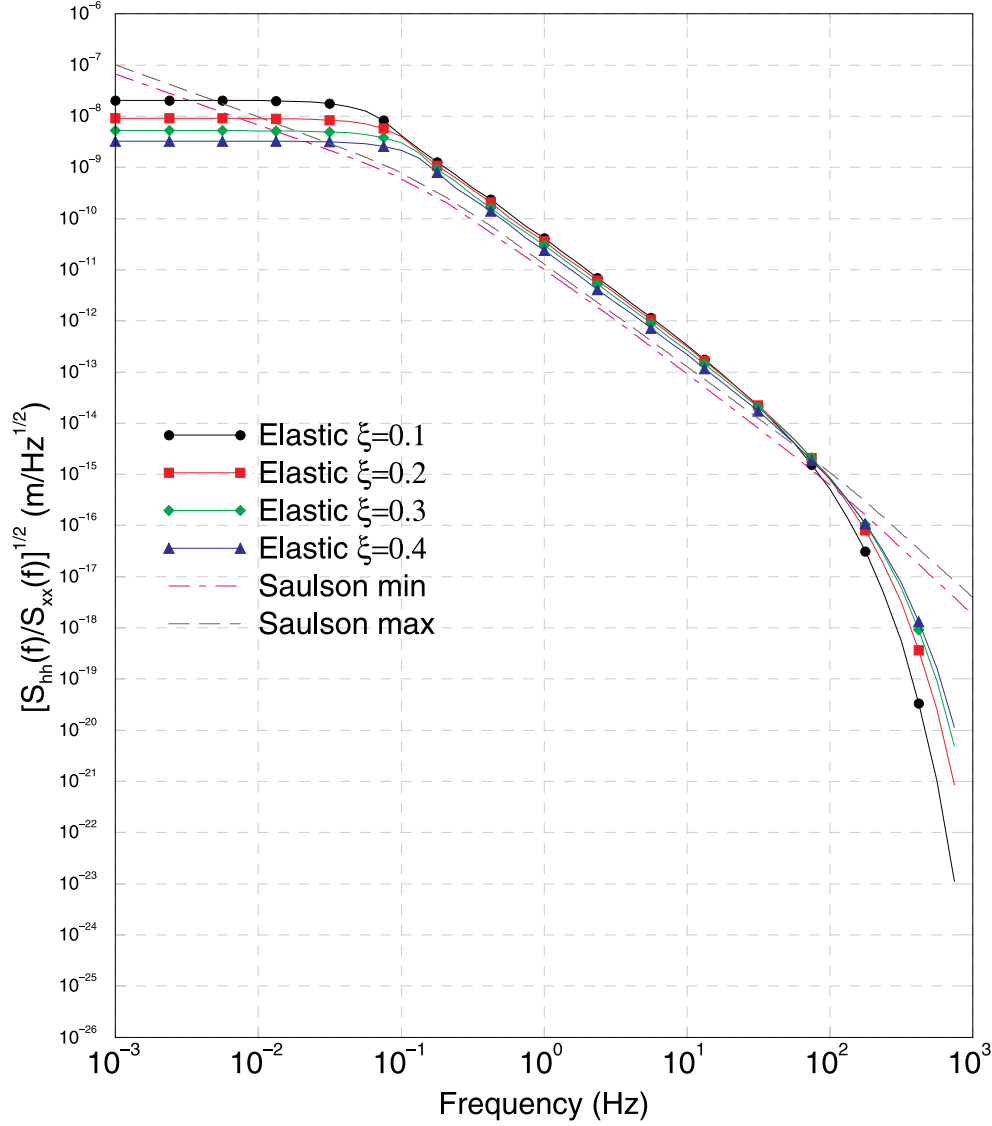
Figure 5. The ratio between the Newtonian noise spectral amplitude $S_{hh}^{1/2}$ and the horizontal seismic noise spectral amplitude $S_{xx}^{1/2}$. We assume that the test masses behave as a free mass, so that $H(\omega) = -\omega^2$. The four full curves are the predictions of the elastic homogeneous model, the slanted curves are the predictions of Saulson's model.

(This figure can be viewed in colour in the electronic version of the article; see http://www.iop.org)

produces the exponential damping visible in the figure, starting from a frequency which can be determined from figure 4(*b*).

3.3. Seismic model validation

The assumptions we made in order to simplify our model have some consequences which can be verified experimentally in an easy enough way. From the isotropy hypothesis only, it follows, for example, that the seismic cross power spectra are zero in the vectorial case, for example, $\langle \delta x_i(r)\, \delta z(r) \rangle = 0$. A similar conclusion is true in the tensorial case for correlations between displacements in perpendicular directions.

If only Rayleigh modes are present we get some quantitative relations between different correlations, which can be easily extracted from equations (63)–(68). In particular, we can write

$$\langle \delta x^2 \rangle = \frac{1}{2}\frac{|u_X|^2}{|u_Z|^2}\langle \delta z^2 \rangle. \tag{73}$$

In order to give a rough estimation of the validity of this relation we have evaluated the power spectra of horizontal and vertical noise using some preliminary measurements in the [0–15] Hz range. The ratio of the two mediated power spectra is plotted versus the frequency in figure 6. As can be seen the ratio is roughly constant for $f < 6$ Hz, while for higher frequencies it rises approximately linearly. We have verified that in this range there is little dependence on the time of the measurement, so we are tempted to conclude that human activity is relevant for seismic noise only for higher frequencies. However these
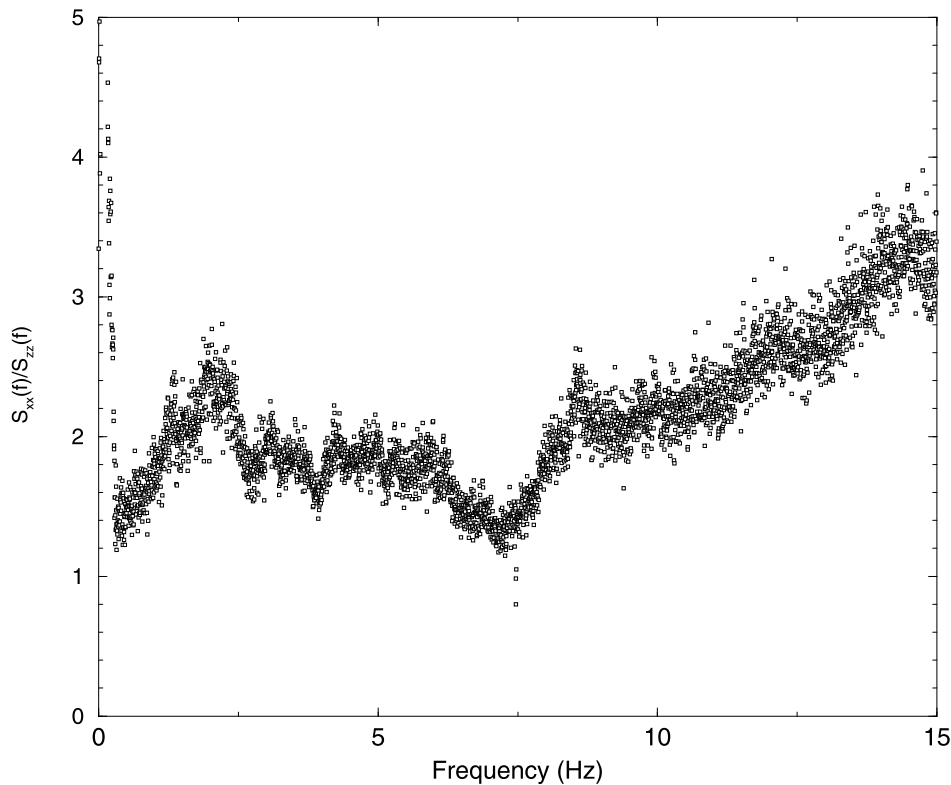
Figure 6. Experimental estimate of the ratio between the horizontal noise power spectrum and the vertical one.

are only very preliminary results. We stress that in order to give a clear validation of our model we need information about cross spectra at a finite distance.

4. Effect of the apparatus infrastructure

In this section we want to make some comments about the effect of the direct gravitational coupling of the mirror to the massive infrastructure of the interferometer.

We start by giving a crude estimate of some of these effects, in particular, of the gravitational coupling to the basement ring and to the tower. Our results will be parametrized in the form of a ratio between the seismic spectrum and the Newtonian noise spectrum. Note that this ratio is not additive with the one obtained in the previous section, because it is strongly correlated with it. The correct procedure would be first to add accelerations and then compute the power spectrum. However, we will not go into these details here, because as we will see the effect of the apparatus infrastructure is an order of magnitude smaller than the direct coupling to the background.

The inverted pendulum was designed as a pre-isolator stage for the horizontal motion [7]: a horizontal table is supported by three elastic legs, which in turn are supported by a rigid common base. The table supports the super-attenuator chain (see figure 7).

4.1. Effect of the basement ring

We assume that the basement of the legs can be modelled as a ring, which can be parametrized in a cylindrical coordinate system as

$$x = R \cos\theta + \delta x + z_0 \delta\theta_y - R \sin\theta \, \delta\theta_z$$
$$y = R \sin\theta + \delta y - z_0 \delta\theta_x + R \cos\theta \, \delta\theta_z \tag{74}$$
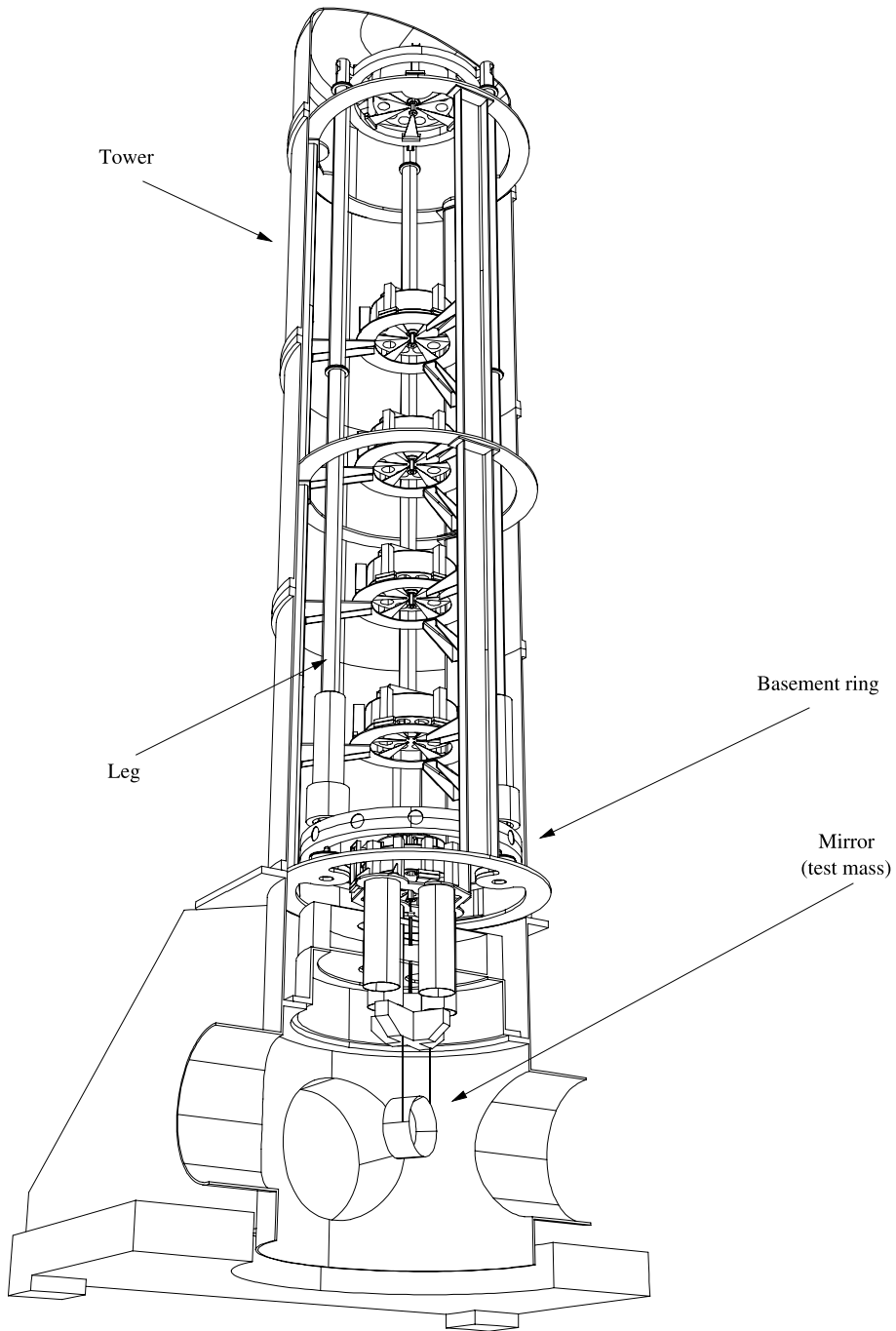$$z = z_0 + \delta z + R \sin\theta \, \delta\theta_x - R \cos\theta \, \delta\theta_y$$

where δx, δy and δz are the horizontal and vertical seismic displacements, $\delta\theta_x$ and $\delta\theta_y$ the tilt angular fluctuations and $\delta\theta_z$ the torsional one. We put the origin of the reference frame in the basement of the tower, and we also assume that the internal modes of the structures are not excited by the seismic motion. For low enough frequencies this will be true, and the structures could be considered as bodies in rigid motion, as in equation (74). Now we evaluate the direct gravitational action of the ring on the mirror suspended in the point $(0, 0, h)$ as the first-order term in the fluctuations of the integral

$$(\delta a_x, \delta a_y, \delta a_z) = G M_{\text{ring}} \int \frac{(x, y, z - h)}{\left[x^2 + y^2 + (z - h)^2\right]^{3/2}} \frac{\mathrm{d}\theta}{2\pi} \tag{75}$$

which gives

$$\begin{pmatrix} \delta a_x \\ \delta a_y \\ \delta a_z \end{pmatrix} = \frac{G M_{\text{ring}}}{\left[R^2 + (z_0 - h)^2\right]^{5/2}} \left\{ \left[(z_0 - h)^2 - \tfrac{1}{2}R^2\right] \begin{pmatrix} \delta x \\ \delta y \\ -\delta z \end{pmatrix} \right.$$
$$\left. + \left[R^2\left(z_0 - \tfrac{3}{2}h\right) + z_0(z_0 - h)^2\right] \begin{pmatrix} \delta\theta_y \\ -\delta\theta_x \\ 0 \end{pmatrix} \right\}. \tag{76}$$

It is interesting to note that the effect of the ring depends qualitatively on its position relative to the mirror. In the case where $R^2 < 2(z_0 - h)^2$ the Newtonian acceleration is in phase with the horizontal seismic displacement, while in the other case it is of opposite sign. This suggests that it is possible to choose the geometry parameters in such a way as to minimize

Figure 7. Schematic view of the superattenuator tower.

the Newtonian effect, if needed. In particular, if we take $R^2 = 2(z_0 - h)^2$ the horizontal and vertical seismic displacement of the ring give no Newtonian noise to first order.

Using the parameters of the final design [8] we obtain the numerical estimate

$$
\begin{pmatrix} \delta a_x \\ \delta a_y \\ \delta a_z \end{pmatrix} = c_1 \begin{pmatrix} \delta x \\ \delta y \\ -\delta z \end{pmatrix} + c_2 \begin{pmatrix} \delta\theta_y \\ -\delta\theta_x \\ 0 \end{pmatrix} \qquad \text{with} \quad c_1 = 0.25 \times 10^{-7}, \quad c_2 = 0.77 \times 10^{-7},
$$

(77)

which can be easily converted to the transfer function for the elastic model

$$
\langle |\delta h(\omega)|^2 \rangle = \frac{4}{L^2 |H(\omega)|^2} \left[c_1^2 + c_2^2 \frac{|u_\theta|^2}{|u_X|^2} \left(\frac{\omega}{c_T} \right)^2 + 2 c_1 c_2 \frac{\mathrm{Re}\,(u_X^\star u_\theta)}{|u_X|^2} \left(\frac{\omega}{c_T} \right) \right]
$$
$$
\times \mathcal{G} \left(\frac{\omega L}{c_T \sqrt{x}} \right) \langle \delta x_i(\omega)^2 \rangle.
$$

(78)

It is interesting to note that the importance of tilt seismic noise grows with the frequency: using the parameters listed in table 1 we see that the transfer function scales as f^{-2} at low frequencies, but start to be proportional to f^{-1} somewhere between 10 Hz (in the low-shear modulus case) and 50 Hz. However, the effect is small: in the low-shear modulus case we can write

$$
\frac{S_{hh}}{S_{xx}} = \frac{4.22 \times 10^{-13}}{f^2} \sqrt{1 + 1.3 \times 10^{-1} f + 4.15 \times 10^{-3} f^2}
$$

(79)

which is more that one order of magnitude smaller than the bulk effect (cf figure 5) in the relevant frequency range.

4.2. Effect of the tower

The tower is composed of two main parts: a higher tower for the implementation of the suspensions and a lower one which houses the payload. The lower tower is a cylindrical tank of $R = 1$ m in radius, 2.74 m in height and 15 mm in thickness. The higher part is constituted by a series of rings of $R = 1$ m in radius and a cupola of 1000 kg in weight, which define the vacuum tank of the suspension. A complete tower is 10.441 m in height and 22 990 kg in weight. Suppose we can model the tower as a cylinder $h = 10.5$ m in height, $R = 1$ m in radius, 22 000 kg in weight and $e = 0.01$ m in thickness; we neglect the effect of the cupola.

We can use equation (76) directly, integrating over z_0 from 0 to h_{tower} after the substitution

$$
M_{\mathrm{ring}} \rightarrow M_{\mathrm{tower}} \frac{\mathrm{d}z_0}{h_{\mathrm{tower}}}
$$

(80)

obtaining

$$
\begin{pmatrix} \delta a_x \\ \delta a_y \\ \delta a_z \end{pmatrix} = -G \frac{M_{\mathrm{tower}}}{h_{\mathrm{tower}}} \left\{ \left[\frac{(h_{\mathrm{tower}} - h)}{2 \left(R^2 + (h_{\mathrm{tower}} - h)^2 \right)^{3/2}} + \frac{h}{2 \left(R^2 + h^2 \right)^{3/2}} \right] \begin{pmatrix} \delta x \\ \delta y \\ -\delta z \end{pmatrix} \right.
$$
$$
\left. + \left[\frac{R^2 + (h_{\mathrm{tower}} - h)^2 + h(h_{\mathrm{tower}} - h)/2}{\left(R^2 + (h_{\mathrm{tower}} - h)^2 \right)^{3/2}} - \frac{R^2 - h^2/2}{\left(R^2 + h^2 \right)^{3/2}} \right] \begin{pmatrix} \delta\theta_y \\ -\delta\theta_x \\ 0 \end{pmatrix} \right\}.
$$

(81)

Numerically this means, with the parametrization in equation (77), $c_1 = -2.51 \times 10^{-8}$, $c_2 = 0.934 \times 10^{-8}$. This relation has the same structure as equation (77), with smaller coefficients so we can conclude that this effect is also negligible. We note that in this case

we know the lowest frequency of the internal modes of the tower, which has been calculated with a finite-element approximation (see [8]) to be around 15 Hz, so we expect our estimate to be realistically below that.

5. Discussion and conclusions

The first point we want to stress is that the conclusions about the amplitude of the Newtonian noise is remarkably model independent over a wide range of frequency: looking at figure 5 we see that between 10^{-1} and 10^2 Hz the different numerical estimates are all of the same order of magnitude. This is important because we do not expect a particular model of seismic motion to capture all the aspects which are potentially relevant.

In some sense the elastic model and Saulson's one can be seen as two extreme possibilities: the first is well founded from a physical point of view, but it assumes a homogeneous medium for the seismic waves, and owing to that cannot take into account coherence loss effects, which can be induced by scattering effects on medium defects. On the other hand, Saulson's model gives strongly uncorrelated ground modes, and it is probably inefficient in accounting for coherence effects.

More refined models are certainly possible, in particular, it is possible to study the modifications of the elastic model induced by inhomogeneities of the medium, but probably the results will not justify the effort. In our opinion the first step is the validation of the models, in particular of the elastic one, which gives a lot of predictions about spatial correlations of linear and angular seismic displacements. In particular, it will be important to test the surface mode dominance approximation we have used, which, as we noted, gives for example a prediction about the absence of torsional noise.

All the power spectra of equations (63)–(68) can be measured potentially at different space separations, and some of these measurements are actually in progress.

What is the relevance of the Newtonian noise from an experimental point of view? The seismic noise spectral amplitude (for coincident points) measured in the interferometer's site can be roughly parametrized, in the frequency range of interest, as

$$\langle \delta x_i(f)^2 \rangle^{1/2} \simeq \frac{10^{-6}}{f^2} \ \text{m Hz}^{-1/2} \tag{82}$$

which, combined with the elastic transfer function we have evaluated, give a Newtonian spectral amplitude of

$$\langle |\delta h(f)|^2 \rangle^{1/2} \simeq 3 \times 10^{-17} \frac{1}{f^4} \tag{83}$$

which is well below the actual sensitivity curve of the VIRGO interferometer, but can become the relevant limitation in the low-frequency range (below 10 Hz) in the final improvement stage.

If the Newtonian noise will become dangerous for the advanced interferometer we stress the concrete possibility of its reduction. An interesting possibility which we have noted in the previous section is to use massive infrastructures of an appropriate geometry to compensate the gravitational fluctuating fields. In our opinion this is an interesting approach which is worth further investigation.

We conclude with two observations.

We have seen that the effect of the direct coupling with the interferometer structures is negligible. In our considerations we limited ourselves to direct coupling of the mirror. This is very reasonable because couplings to other stages are damped by the superattenuator

stages. A possible exception is the marionetta, which is located at a very small distance from the tower structures. The only attenuation of this direct action is provided by the wires which suspend the mirror, so the final effect could be relevant.

Another point is connected to the approximation we have used for the mechanism of coupling between the ground and the interferometer structures. We have imagined the base as a rigid body which follows the 'rigid' part of the surface motion, neglecting the effect of the weight of the structures and the details of the coupling between the base and the ground, which is probably inaccurate.

We will address these questions in a future work.

Acknowledgments

Appendix A. Classification of seismic background waves

In order to obtain an estimate of the seismic noise we want now to simulate the ground as a homogeneous medium limited by the $z = 0$ plane. The general free ground motion can be expanded in elastic waves, which are solutions of the equation [10]

$$\partial_t^2 u_i(x, t) = c_T^2 \partial_k \partial_k u_i(x, t) + (c_L^2 - c_T^2) \partial_i \partial_k u_k(x, t). \tag{A1}$$

These solutions represent longitudinal waves with speed c_L and transverse ones with speed c_T. The field $u_i(x, t)$ represents the displacement of a point from its original position x in direction i.

We take advantage of the symmetries of the problem by separating the displacement field u in the component $\vec{u}$ parallel to the $z = 0$ plane and in the component u_z perpendicular to it, and by Fourier transforming in the x, y, t variables.

The boundary conditions are appropriate for a free surface, so that for the stress tensor σ_{ij} must be

$$\sigma_{xz}(x, y, 0) = \sigma_{yz}(x, y, 0) = \sigma_{zz}(x, y, 0) = 0. \tag{A2}$$

We can satisfy these conditions over-imposing some plane-wave solutions with the same frequency ω and the same projection $\vec{k} = (k_x, k_y)$ of the wavevector in the plane $z = 0$. The most general combination with these properties can be written as

$$u(\vec{k}, z, \omega) = \begin{pmatrix} \vec{u} \\ u_z \end{pmatrix} = \epsilon^{(L,+)} \mathrm{e}^{\mathrm{i}k_L z} + \epsilon^{(T,+)} \mathrm{e}^{\mathrm{i}k_T z} + \epsilon^{(L,-)} \mathrm{e}^{-\mathrm{i}k_L z} + \epsilon^{(T,-)} \mathrm{e}^{-\mathrm{i}k_T z} \tag{A3}$$

with

$$k^2 + k_T^2 = \frac{\omega^2}{c_T^2}, \qquad k^2 + k_L^2 = \frac{\omega^2}{c_L^2}. \tag{A4}$$

We use the parametrization

$$\epsilon^{(L,+)} = \alpha \begin{pmatrix} \vec{k} \\ k_L \end{pmatrix}, \qquad \epsilon^{(T,+)} = \beta \begin{pmatrix} -k_T \hat{k} \\ |k| \end{pmatrix} + \gamma \begin{pmatrix} \epsilon \vec{k} \\ 0 \end{pmatrix},$$

$$\epsilon^{(L,-)} = \alpha' \begin{pmatrix} \vec{k} \\ -k_L \end{pmatrix}, \qquad \epsilon^{(T,-)} = \beta' \begin{pmatrix} k_T \hat{k} \\ |k| \end{pmatrix} + \gamma' \begin{pmatrix} \epsilon \vec{k} \\ 0 \end{pmatrix}, \tag{A5}$$

where $\alpha, \beta, \gamma, \alpha', \beta', \gamma'$ are complex amplitudes, and only the real part of equation (A3) is of physical significance. The polarizations $\epsilon^{(L,+)}$ and $\epsilon^{(L,-)}$ label the two longitudinal modes, and are parallel to the wavevector, while $\epsilon^{(T,+)}$ and $\epsilon^{(T,-)}$ label the four transverse modes and are perpendicular to the wavevector.

The conditions (A2) rewritten for the displacement field become

$$iku_z + \partial_z u_x = 0$$
$$\partial_z u_y = 0 \tag{A6}$$
$$c_L^2 \partial_z u_z + ik(c_L^2 - 2c_T^2)u_x = 0$$

where without loss of generality we took $\vec{k} = k\hat{x}$. Using the parametrization (A5) we obtain the conditions

$$kk_T(\gamma - \gamma') = 0$$
$$2kk_L(\alpha - \alpha') + (k^2 - k_T^2)(\beta + \beta') = 0 \tag{A7}$$
$$(k^2(c_L^2 - 2c_T^2) + c_L^2 k_L^2)(\alpha + \alpha') + 2c_T^2 kk_T(\beta - \beta') = 0.$$

In the particular case $k = 0$ these conditions simplify,

$$\beta + \beta' = 0, \qquad \alpha + \alpha' = 0 \tag{A8}$$

and the combination (A3) decomposes in two independent modes: a longitudinal wave and a transverse one with a wavevector perpendicular to the plane, completely reflected by it.

In the $k \neq 0$ case we can use the conditions (A7) to reduce the independent parameters of the general solution (A3). It is convenient to rewrite it in the form

$$\begin{pmatrix} \vec{u}(\vec{k}, z, \omega) \\ u_z(\vec{k}, z, \omega) \end{pmatrix} = \sum_\mu \left\{ A_\mu(\vec{k}, \omega) \begin{pmatrix} \vec{k} \cos k_L z - k_T f_2 \hat{k} \cos k_T z \\ ik_L \sin k_L z + ik f_2 \sin k_T z \end{pmatrix} \right.$$
$$+ B_\mu(\vec{k}, \omega) \begin{pmatrix} i\vec{k} \sin k_L z - ik_T f_1 \hat{k} \sin k_T z \\ k_L \cos k_L z + k f_1 \cos k_T z \end{pmatrix}$$
$$\left. + C_\mu(\vec{k}, \omega) \begin{pmatrix} \epsilon \vec{k} \cos k_T z \\ 0 \end{pmatrix} \right\}. \tag{A9}$$

Here we have introduced the convenient parametrization $A = \alpha + \alpha'$, $B = \alpha - \alpha'$ and $C = \gamma + \gamma'$, while the parameters f_1, f_2 are defined as

$$f_1 = \frac{2kk_L}{k_T^2 - k^2}, \qquad f_2 = \frac{(2c_T^2 - c_L^2)k^2 - c_L^2 k_L^2}{2c_T^2 kk_T}. \tag{A10}$$

This is not the end of the story, because we must impose the regularity of the solution in the $z \to -\infty$ case.

If $k^2 < \omega^2/c_L^2 < \omega^2/c_T^2$ both k_L and k_T are real, so there are no additional constraints and we get three independent modes. The piece proportional to C gives a purely transverse mode which is the superposition of an incident and a completely reflected wave, for $k^2 = \omega^2/c_T^2$ the total wavevector becomes completely parallel to the $z = 0$ plane end. With reference to figure 3 we label this mode with $\mu = 0$. The pieces proportional to A and B represent two independent superpositions of transverse and longitudinal modes which can be separated in the following convenient way.

(i) A purely longitudinal incident wave, which is reflected by the $z = 0$ plane as a superposition of a transverse and a longitudinal wave. The absence of the longitudinal incident wave ($\beta = 0$) gives the constraint $A_\mu = -(f_1/f_2)B_\mu$. We label this mode with $\mu = 1$.

(ii) A purely transverse incident wave. As in the first case, the outgoing wave is the superposition of a longitudinal and a transverse wave, and we get the constraint $A_\mu = -B_\mu$ ($\alpha = 0$). We label this mode with $\mu = 2$.

If $\omega^2/c_L^2 < k^2 < \omega^2/c_T^2$ k_T is real but k_L is imaginary. In order to exclude the unphysical exponentially growing solution we need the additional condition $A_\mu = -B_\mu$. The pieces proportional to A and B are no longer independent and we get only a mode, which we label with $\mu = 3$, which can be described as a purely transverse incident wave which is reflected as a superposition of a transverse outgoing wave and a surface wave exponentially damped with the depth. The C piece is independent of k_L, so the $\mu = 0$ mode is admissible in this interval, for a total of two independent modes.

The last case corresponds to $\omega^2/c_T^2 < k^2$. Both k_L and k_T are imaginary, so we need the two additional conditions $\alpha = 0$ and $\beta = 0$ (which means $A_\mu = -B_\mu$ and $f_1 = f_2$). The system (A7) becomes homogeneous in α, β, and is soluble if its determinant is zero, which gives the condition

$$x^3 - 8x^2 + 8x(3 - 2\xi) + 16(\xi - 1) = 0, \qquad 0 < x < 1, \qquad x = \frac{\omega^2}{k^2 c_T^2}, \qquad \text{(A11)}$$

where ξ is the square of the ratio between the transverse and longitudinal speed of the wave

$$\xi = \frac{c_T^2}{c_L^2}, \qquad 0 < \xi < \tfrac{1}{2}. \qquad \text{(A12)}$$

There is only one solution of equation (A11), for a given value of ξ, which corresponds to a surface wave superposition of a longitudinal and a transverse mode, both exponentially damped with the depth (Rayleigh waves).

As discussed in the text this is probably the more important mode from a practical point of view, and we label it with $\mu = 4$. The transverse mode proportional to C is clearly not admissible (see figure 3 for reference).

The key point of our work is that the Newtonian accelerations can also be expressed as linear functions of the amplitudes A_μ, B_μ and C_μ, so if we express these as functions of the seismic displacements we can obtain a 'transfer function' which connects seismic and Newtonian noise.

We are particularly interested in the $\mu = 4$ mode, so we specialize to this case. The modulus of the vector $\vec{k}$ is fixed in a unique way by ω, so at fixed frequency we sum only over the directions $\hat{k}$, obtaining

$$\vec{u}(x, \omega) = \sum_{\hat{k}} A_4(\hat{k}, \omega)\hat{k}\left(k e^{ik_L z} - 2k \frac{k_L k_T}{k_T^2 - k^2} e^{ik_T z}\right) e^{i\vec{k}\vec{x}} \qquad \text{(A13)}$$

$$u_z(x, \omega) = \sum_{\hat{k}} A_4(\hat{k}, \omega)\left(k_L e^{ik_L z} + 2k_L \frac{k^2}{k_T^2 - k^2} e^{ik_T z}\right) e^{i\vec{k}\vec{x}} \qquad \text{(A14)}$$

with

$$k = \frac{\omega}{c_T}\sqrt{\frac{1}{x}}, \qquad k_L = -i\frac{\omega}{c_T}\sqrt{\frac{1}{x} - \xi}, \qquad k_T = -i\frac{\omega}{c_T}\sqrt{\frac{1}{x} - 1}. \qquad \text{(A15)}$$

Appendix B. Sum over modes

If we restrict the sum over modes to the surface ones only, it is possible to evaluate it in closed form if we assume isotropy of the correlation functions. The result can be expressed

in terms of Bessel functions as follows:

$$G^S(\vec{x}_1, \vec{x}_2) = J_0\left(\frac{\omega}{c_T\sqrt{x}}|x_1 - x_2|\right) \tag{B1}$$

$$G_x^V(\vec{x}_1, \vec{x}_2) = J_1\left(\frac{\omega}{c_T\sqrt{x}}|x_1 - x_2|\right)\cos(\theta_{12}) \tag{B2}$$

$$G_y^V(\vec{x}_1, \vec{x}_2) = J_1\left(\frac{\omega}{c_T\sqrt{x}}|x_1 - x_2|\right)\sin(\theta_{12}) \tag{B3}$$

$$G_{xx}^T(\vec{x}_1, \vec{x}_2) = \frac{1}{2}J_0\left(\frac{\omega}{c_T\sqrt{x}}|x_1 - x_2|\right) - \frac{1}{2}J_2\left(\frac{\omega}{c_T\sqrt{x}}|x_1 - x_2|\right)\cos(2\theta_{12}) \tag{B4}$$

$$G_{yy}^T(\vec{x}_1, \vec{x}_2) = \frac{1}{2}J_0\left(\frac{\omega}{c_T\sqrt{x}}|x_1 - x_2|\right) + \frac{1}{2}J_2\left(\frac{\omega}{c_T\sqrt{x}}|x_1 - x_2|\right)\cos(2\theta_{12}) \tag{B5}$$

$$G_{xy}^T(\vec{x}_1, \vec{x}_2) = -\frac{1}{2}J_2\left(\frac{\omega}{c_T\sqrt{x}}|x_1 - x_2|\right)\sin(2\theta_{12}). \tag{B6}$$

Here we have defined the angle θ_{12} which is the direction of the vector $\vec{x}_1 - \vec{x}_2$ in the chosen reference frame. The spatial dependence of a correlation function is completely determined by its transformation properties under rotation.

References

[1] Brune J N and Oliver J 1959 The seismic noise of the Earth's surface *Bull. Am. Seism. Soc.* **49** 349–53

[2] Fix J E 1972 Ambient earth motion in the periodic range from 0.1 to 2560 seconds *Bull. Am. Seism. Soc.* **62** 1753–60

[3] Iyer H M 1970 Seismology *Global Geophysics* ed R H Tucker, A H Cook, H M Iyer and F D Stacey (English Universities Press)

[4] Carter J A, Barstow N, Pomeroy P W, Chael E P and Leahy P J 1991 High frequency seismic noise as a function of the depth *Bull. Am. Seism. Soc.* **81** 1101–14

[5] Saulson P R 1984 Terrestrial gravitational noise on a gravitational wave antenna *Phys. Rev.* D **30** 732–6

[6] Saulson P R 1994 *Fundamentals of Interferometric Gravitational Wave Detectors* (Singapore: World Scientific)

[7] De Salvo R, Gaddi A, Gennaro G, Holloway L, Losurdo G and Winterflood J 1996 A proposal for a pre-isolator stage for the Virgo superattenuator *Virgo Note* 96/034

[8] The VIRGO collaboration 1997 *Final Design Report* VIR-TRE-1000-13

[9] Verkindt D 1993 Gravitational noise on Virgo mirrors *Virgo Note* 93/019

[10] Love A E H 1944 *A Treatise on the Mathematical Theory of Elasticity* 4th edn (New York: Dover)

[11] Doyle H 1995 *Seismology* (Chichester: Wiley)

[12] Hughes S A and Thorne K S 1998 *Phys. Rev.* D submitted
        Hughes S A and Thorne K S 1998 Seismic gravity-gradient noise in interferometric gravitational-wave detectors *Caltech preprint* GRP-500 (*Phys. Rev.* D submitted)